

# Dishevelled-1 Regulates Microtubule Stability: A New Function Mediated by Glycogen Synthase Kinase-3 $\beta$

Olga Krylova,<sup>\*‡</sup> Marcus J. Messenger,<sup>\*</sup> and Patricia C. Salinas<sup>\*‡</sup>

<sup>\*</sup>The Randall Institute, King's College London, London, United Kingdom, WC2B 5RL; and <sup>‡</sup>Department of Biochemistry, Imperial College of Science, Technology and Medicine, London, United Kingdom, SW7 2AY

**Abstract.** Dishevelled has been implicated in the regulation of cell fate decisions, cell polarity, and neuronal function. However, the mechanism of Dishevelled action remains poorly understood. Here we examine the cellular localization and function of the mouse Dishevelled protein, DVL-1. Endogenous DVL-1 colocalizes with axonal microtubules and sediments with brain microtubules. Expression of DVL-1 protects stable microtubules from depolymerization by nocodazole in both dividing cells and differentiated neuroblastoma cells. Deletion analyses reveal that the PDZ domain, but not the DEP domain, of DVL-1 is required for microtubule

stabilization. The microtubule stabilizing function of DVL-1 is mimicked by lithium-mediated inhibition of glycogen synthase kinase-3 $\beta$  (GSK-3 $\beta$ ) and blocked by expression of GSK-3 $\beta$ . These findings suggest that DVL-1, through GSK-3 $\beta$ , can regulate microtubule dynamics. This new function of DVL-1 in controlling microtubule stability may have important implications for Dishevelled proteins in regulating cell polarity.

**Key words:** WNT • granule cells • cerebellum • cytoskeleton • nocodazole

## Introduction

Dishevelled was originally characterized as a *Drosophila* mutation that affects planar polarity and epithelial patterning in the early embryo (Perrimon and Mahowald, 1987; Adler, 1992; Klingensmith et al., 1994). Dishevelled is a cytoplasmic protein implicated in the Notch and WNT signaling pathways. In the Notch pathway, Dishevelled acts as a repressor, whereas it is a positive regulator of the WNT signaling pathway (Klingensmith et al., 1994; Noordermeer et al., 1994; Siegfried et al., 1994; Axelrod et al., 1996). In *Drosophila* and *Xenopus* embryos, overexpression of *dishevelled* confers a similar phenotype to *Wnt* overexpression, suggesting that Dishevelled activates WNT signaling (Rothbacher et al., 1995; Sokol et al., 1995; Yanagawa et al., 1995). The current model for the canonical pathway proposes that Wg, the *Drosophila* homologue of WNT, activates Dishevelled through the Frizzled receptor to control epithelial patterning in *Drosophila*. Activation of Dishevelled results in the inhibition of Shaggy (Sgg), a serine/threonine kinase, and the homologue of glycogen synthase

kinase-3 $\beta$  (GSK-3 $\beta$ ).<sup>1</sup> Inhibition of GSK-3 $\beta$ /Sgg leads to increased levels of  $\beta$ -catenin/Armadillo and the activation of transcription via T-cell factor/Pangolin factors (Cadigan and Nusse, 1997; Arias et al., 1999). In planar cell polarity, however, Dishevelled activates the c-Jun NH<sub>2</sub>-terminal protein kinase (JNK) pathway in an Armadillo-Pangolin-independent manner (Boutros et al., 1998). Different domains of Dishevelled are required for signaling through these different pathways. It has been proposed that Dishevelled function is to interpret signals coming from the plasma membrane and to direct them to different signaling pathways (Boutros and Mlodzik, 1999).

Dishevelled proteins possess three conserved domains: a DIX domain, present in the WNT antagonizing protein Axin (Zeng et al., 1997), a PDZ domain involved in protein-protein interactions (Ponting et al., 1997), and a DEP domain found in proteins that regulate Rho GTPases (Ponting and Bork, 1996). In the canonical WNT pathway, the PDZ domain is required. Whereas the DEP domain is

Drs. Krylova and Messenger contributed equally to this work and should be considered co-first authors.

Address correspondence to Patricia C. Salinas, Department of Biochemistry, Imperial College of Science, Technology and Medicine, London SW7 2AY. UK. Tel.: 44 020 7594 5208. Fax: 44 020 7594 5207. E-mail: p.salinas@ic.ac.uk

<sup>1</sup>Abbreviations used in this paper: CNS, central nervous system; DVL, mouse Dishevelled; EGL, external granular layer; GAP-43, growth associated protein-43; GFP, green fluorescence protein; GSK-3 $\beta$ , glycogen synthase kinase-3 $\beta$ ; GST, glutathione S-transferase protein; HA, hemagglutinin; IGL, internal granular cell layer; JNK, c-Jun NH<sub>2</sub>-terminal protein kinase; MAP, microtubule-associated protein; MT, microtubule; NB2a, neuroblastoma 2a.

essential for activation of the planar polarity pathway (for review, see Boutros and Mlodzik, 1999). Mutation in the DEP domain of *dishevelled* results in the random orientation of hair cells, suggesting that Dishevelled may control the reorganization of the cytoskeleton in planar cell polarity (Axelrod et al., 1998). Epistatic analyses support the role of RhoA in this process (Strutt et al., 1997). Thus, Dishevelled may regulate the actin cytoskeleton through the JNK pathway. However, the role of Dishevelled in regulating the cytoskeleton through other pathways has not been established.

In the mouse, three *Dishevelled* genes, *Dvl-1*, *Dvl-2*, and *Dvl-3* have been identified (Sussman et al., 1994; Klingensmith et al., 1996; Yang et al., 1996). *Dvl-3* is expressed throughout development, but functional studies are missing (Tsang et al., 1996). *Dvl-2* is ubiquitously expressed during embryonic development and in many adult tissues (Klingensmith et al., 1996). More recently, *Dvl-2* has been shown to be highly expressed in the outer root sheath and hair precursor cells (Millar et al., 1999). Studies using transgenic mice show that mouse Dishevelled protein, DVL-2, mimics WNT-3 function and therefore suggest that DVL-2 is part of the WNT signaling pathway involved in hair development (Millar et al., 1999). Like *Dvl-2*, *Dvl-1* is ubiquitously expressed at early stages of development (Sussman et al., 1994). In the central nervous system (CNS), *Dvl-1* is highly expressed in areas of high neuronal density at embryonic and postnatal stages of development (Sussman et al., 1994). Analysis of the *Dvl-1* null mouse shows that *Dvl-1* is not required for early development. However, *Dvl-1* null mice exhibit behavioral abnormalities and neurological deficits, suggesting that DVL-1 is required for the formation and/or function of specific neuronal pathways (Lijam et al., 1997).

Neurons are highly polarized cells with stereotypic dendritic arborizations and axons. The neuronal cytoskeleton is essential for the formation and maintenance of this polarized morphology. Recent studies on cerebellar neurons have demonstrated that WNT-7a regulates axonal morphology. WNT-7a increases growth cone size and axonal branching, while decreasing axon length (Lucas and Salinas, 1997; Hall et al., 2000). These changes are mediated through the inhibition of GSK-3 $\beta$ . The axonal remodeling activity of WNT-7a is associated with changes in microtubule (MT) organization (Hall et al., 2000), and the GSK-3 $\beta$ -mediated phosphorylation of the microtubule-associated protein, MAP-1B (Lucas et al., 1998). GSK-3 $\beta$  also phosphorylates Tau, an axonal microtubule-associated protein that, like MAP-1B, is involved in MT stability (Hanger et al., 1992). These findings suggest that GSK-3 $\beta$  regulates the organization of neuronal MTs by changing the phosphorylation of MAPs. However, the mechanisms controlling GSK-3 $\beta$  activity during MT reorganization remain poorly understood.

Here we examine the expression and function of DVL-1, a regulator of GSK-3 $\beta$ , in developing neurons. In the CNS, DVL-1 is localized to neurons of the cortex, hippocampus, pons, and cerebellum. Three isoforms of DVL-1 are differentially expressed during neuronal maturation. DVL-1 colocalizes with axonal MTs and sediments with brain MTs. Expression of DVL-1 protects stable MTs from de-

polymerization by nocodazole. The PDZ domain and, to a lesser extent, the DIX domain of DVL-1 are required for MT stabilization. Furthermore, this process is mediated by the inhibition of GSK-3 $\beta$ . These findings demonstrate a novel function for DVL-1 in regulating MT organization.

## Materials and Methods

### Production of DVL-1 Antibodies

Polyclonal DVL-1 antibody was made against the carboxy-terminal 46 amino acids of DVL-1 fused to glutathione S-transferase protein (GST-DVL-46; kindly provided by Karl Willert and Roel Nusse, Stanford University, Stanford, CA). Specific DVL-1 antibody was affinity purified using CNBr-Sepharose bead coupled to GST-DVL-46. The obtained antiserum was run through a GST column, and then affinity purified on a GST-DVL-46 column (Pierce Chemical Co.). This antibody, but not the preimmune serum, recognized the DVL-1 protein in Western blots. Antibody specificity was confirmed by the lack of DVL-1 immunoreactivity in cerebellar protein extracts isolated from the *DVL-1* null mutant mice (Lijam et al., 1997) and by blocking with purified GST-DVL-46 peptide.

### Neuronal Cell Cultures

Cerebellar granule cells were isolated from newborn mice and purified using Percoll gradients (Hatten, 1985). Neurons were plated onto laminin-coated dishes at a density of  $10^5$  cells/cm<sup>2</sup> and grown in serum-free medium for 2 d, as described previously (Lucas et al., 1998). Cells were fixed either in 4% formaldehyde in PBS or in 3% paraformaldehyde, 0.2% glutaraldehyde, 0.2% Triton X-100, 10 mM EGTA in PBS (detergent fixation) and stored in PBS at 4°C.

### Immunofluorescence Microscopy

Fixed cultures were incubated with primary antibodies overnight at 4°C. Goat anti-rabbit IgG and goat anti-mouse IgG antibodies labeled with Alexa 568 and Alexa 488, respectively (Molecular Probes), and anti-rat IgG-FITC from Vector or anti-rat IgG-AMCA (Chemicon) were used as secondary antibodies. Images were obtained with a microscope (BX60; Olympus) or with a laser scanning confocal microscope (DMR; Leica). Photographic images were scanned, stored as TIFF files, and analyzed using Photoshop 4.0 (Adobe Systems Inc.). Other primary antibodies used were against acetylated tubulin (Sigma-Aldrich), growth associated protein-43 (GAP-43; monoclonal, Boehringer; polyclonal from Dr. Graham Wilkin, Imperial College, London, UK), and hemagglutinin (HA; Boehringer). For immunohistochemistry, brain tissues were fixed with 4% paraformaldehyde (PFA), embedded in polyfreeze tissue embedding medium (Polysciences, Inc.), and stored at -70°C. Cryosections of 18  $\mu$ m were fixed again in 4% PFA and incubated with DVL-1 antibody overnight. Antibody was visualized with the ABC kit (Vector Laboratories) and DAB. No staining was obtained with DVL-1 antibody previously blocked with purified GST-DVL-46 peptide.

### Taxol Polymerization and Cycling of Microtubules

For taxol experiments, crude MTs were prepared from mouse cerebellum using a method adapted from Fujii et al. (1990). Dissected cerebella were homogenized on ice in MES buffer (100 mM MES, pH 6.5, 0.5 mM magnesium acetate, 1 mM dithiothreitol, 1 mM EGTA, 100  $\mu$ g/ml PMSF, 10  $\mu$ g/ml aprotinin, 10  $\mu$ g/ml pepstatin, and 10  $\mu$ g/ml leupeptin) and centrifuged at 4°C for 40 min at 180,000 g. The supernatant was removed and incubated with 10  $\mu$ M taxol and 1 mM GTP at 37°C for 30 min to polymerize the MTs. The sample was then centrifuged at 100,000 g for 30 min at 25°C to recover the crude MT pellet, which was then resuspended in gel loading buffer.

In MT cycling experiments, crude MT protein from mouse brain was cycled twice through successive rounds of MT assembly and disassembly. In brief, whole mouse brain was homogenized in PEM buffer (100 mM PIPES, pH 6.8, 2 mM EGTA, 1 mM MgCl<sub>2</sub>) with 1 mM ATP and 0.1 mM GTP. After centrifugation at 100,000 g for 1 h at 4°C, the homogenate was added to an equal volume of PEM buffer containing 8 M glycerol, 1 mM ATP, and 1 mM GTP. The solution was incubated at 37°C for 30 min and spun again for 1 h at room temperature to collect the polymerized MT

fraction (P1) and supernatant (S1). MTs were depolymerized by incubating on ice for 1 h, and then spun down at 100,000 *g*, 4°C, to collect the cold stable MT fraction (CSP1). The supernatant was then incubated at 37°C for 30 min to polymerize MTs again, and spun down to obtain supernatant (S2) and MT pellet (P2). The P2 fraction was then subjected to a further cycle of temperature-dependent depolymerization and repolymerization. In a second set of experiments, DVL-HA, obtained from cell lysates of DVL-HA-transfected COS cells, was added to the crude MT suspension before two successive cycles of cold/warm exposure. Aliquots were removed for Western analysis. Endogenous DVL-1 protein was detected with DVL-1 antibody and DVL-HA with the HA antibody.

### Western Blot Analysis

Mouse cerebella or whole brains were dissected and homogenized in cold sample buffer. Boiled tissue samples or cultured cell extracts were run on 10% SDS-PAGE gels and proteins were transferred to Hybond-C super (Amersham Pharmacia Biotech) membranes and probed with antibodies against DVL-1, MAP-1B (kindly provided by P. Gordon-Weeks, King's College, London, UK),  $\alpha$ -tubulin, and extracellular signal-regulated kinase (Erk), and developed using HRP-coupled anti-rabbit (Sigma-Aldrich) or anti-mouse (Amersham Pharmacia Biotech) antibodies and electrochemiluminescence reagent (Pierce Chemical Co.). Protein levels were normalized using the BSA protein assay (Pierce Chemical Co.) and Coomassie blue or by staining the membranes with Ponceau red.

### Plasmids and Transfections

DVL-HA, DVL-1 deletion mutants, and GSK-3 $\beta$ -HA constructs were generated by PCR using the high fidelity thermostable DNA polymerase plaque-forming units (Stratagene or Promega) and cloned into the pCS2+ expression vector. Constructs were verified by DNA sequencing. The expression of green-fluorescent protein (GFP), DVL-HA constructs, and GSK-3 $\beta$ -HA were driven by the cytomegalovirus promoter. DVL-1, without the tag, was driven by the SV40 promoter. Plasmids for transfection were isolated using a maxi-prep endotoxin-free kit (QIAGEN). COS cells were transfected using the calcium-phosphate technique and cultured for another 48 h. Neuroblastoma 2a (NB2a) cells were transfected using Lipofectamin (GIBCO-BRL), and then differentiated for 48 h in the presence of 1 mM dibutyryl-cyclic-AMP. Cells were treated

with nocodazole (10 or 5  $\mu$ M) for 1 h and fixed in 3% formaldehyde, 0.2% glutaraldehyde, 0.2% Triton X-100, and 10 mM EGTA in PBS.

## Results

### DVL-1 Is Expressed during Postnatal Development

To examine the function of DVL-1 in neuronal development, we generated an affinity-purified polyclonal antibody against a peptide encoding the 46 carboxy-terminal amino acids of DVL-1. Using this antibody, we found that DVL-1 is localized to several neuronal populations of the adult mouse CNS. High levels of DVL-1 protein were found in neurons of the cerebral cortex, hippocampus, pons, and cerebellum (Fig. 1, A–J). In the cortex, DVL-1 is localized to the cell body and processes of neurons (Fig. 1 A). High levels of DVL-1 were found in pyramidal neurons (Fig. 1 A, insert). In the cerebellum, we examined in more detail the distribution of DVL-1 during postnatal cerebellar development (Fig. 1, D–J). At birth, DVL-1 was found in the external granular cell layer (EGL) and in the forming internal granule cell layer (IGL) of the cerebellum (Fig. 1 D). At P7, the level of DVL-1 is higher in the EGL as granule cells migrate to the IGL. DVL-1 was also observed in the forming IGL (Fig. 1 E). By P14, DVL-1 is highly expressed in the granule cell layer and this expression is maintained in adult life (Fig. 1, F–J). DVL-1 is also expressed in the Purkinje cell layer, when Purkinje cells begin to mature and develop a complex dendritic tree (Fig. 1, F–J). From P21, low levels of DVL-1 were found in the molecular layer (Fig. 1, G–I). In *Dvl-1* null mutant mice, no immunoreactivity was observed (Fig. 1 K). Preincubation of the antibody with the DVL-46 peptide completely

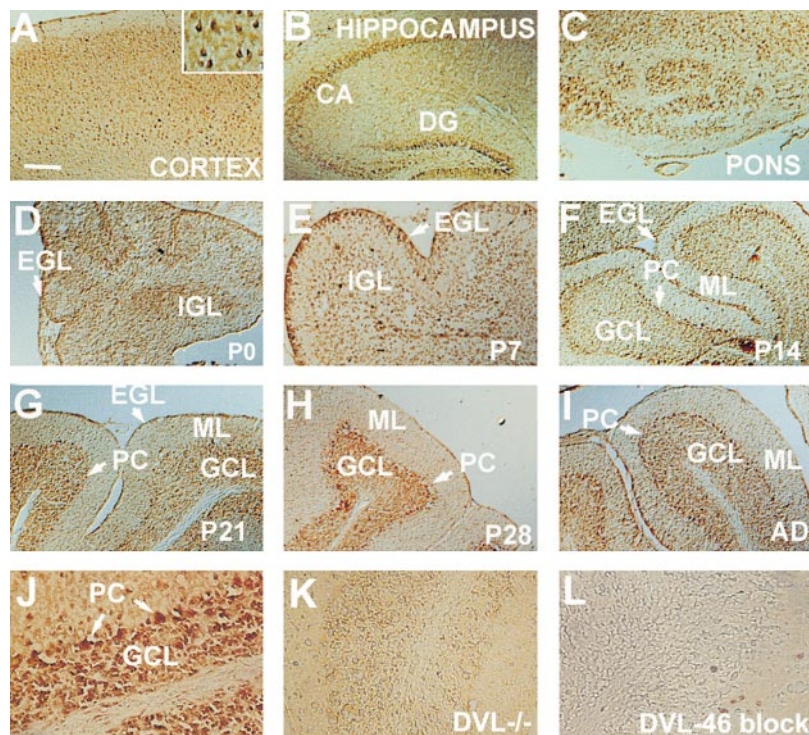


**Figure 1.** DVL-1 expression in postnatal mouse brain. Brain sections were immunostained for DVL-1 (A–J). The highest level of DVL-1 was detected in neurons of the cerebral cortex, hippocampus, pons, and cerebellum (A–C and I). (A, inset) DVL-1 localization in cell bodies and processes of pyramidal neurons. In P0 cerebellum, DVL-1 is expressed in the EGL and forming IGL (D). At P7, DVL-1 immunoreactivity increases in the EGL (E). At P14, DVL-1 was mainly localized in the granule cell layer (GCL) and in the Purkinje cell (PC) layer (F). This pattern of DVL-1 expression was maintained throughout life (G–I). A low level of DVL-1 expression was detected in the molecular layer (ML) from P21 (G–I). At P21, DVL-1 is mainly localized in granule cells and Purkinje cells cell bodies, as shown at higher magnification (J). No immunoreactivity was detected in the cerebellum of adult *Dvl-1* null mutant mice (K). Preincubation of the antibody with DVL-46 peptide completely abolished immunostaining in adult cerebellum (L). AD, adult; DG, dentate gyrus. Bar, 100  $\mu$ M.

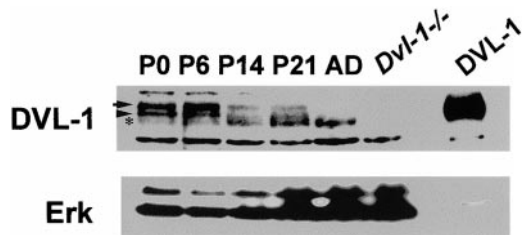


**Figure 2.** DVL-1 isoforms are developmentally regulated. Western blot analysis of cerebellar extracts from P0, P6, P14, P21, and adult mice reveals changes in the level of three DVL-1 isoforms. DVL-1 antibody recognizes three DVL-1 species of 96 kD (arrow), 88 kD (arrowhead), and 83 kD (asterisk). At birth, the three forms of DVL-1 are present, but the 83-kD isoform is expressed at low levels. During cerebellar maturation, expression of the 83-kD isoform increases, while the two higher molecular weight isoforms decrease. Cerebella samples from *Dvl-1* null mutant mice, used as a negative control, reveal the absence of the three DVL-1 isoforms. Expression of DVL-1 in QT-6 cells reveals the presence of the high molecular weight isoforms (DVL-1). The same blot was reprobed with an antibody against extracellular signal-regulated kinase to control for loading.

abolishes DVL-1 staining in adult mouse cerebellum (Fig. 1 L). These results show that DVL-1 is mainly localized to neurons throughout life.

We next examined the levels of DVL-1 in the developing cerebellum by Western analysis. The DVL-1 antibody recognizes three main species migrating with apparent molecular weights of 96, 88, and 83 kD. None of the three species were detected in cerebellar samples isolated from *Dvl-1* null mice, confirming the specificity of our antibody (Fig. 2). The three species of DVL-1 are developmentally regulated. The 96- and 88-kD proteins are present at birth, but their expression declines as development progresses (Fig. 2). In contrast, the lowest molecular weight form (83 kD) increases from P0 to adulthood (Fig. 2). These changes in the mobility of DVL-1 correlate with neuronal maturation, a process characterized by axonal extension and the formation of dendritic arborizations and synapses.

#### *DVL-1 Colocalizes with Axonal Microtubules*

To determine the localization of DVL-1 in neurons, we examined DVL-1 in cerebellar granule cell cultures. Double labeling for GAP-43, a protein that reveals neuronal morphology, shows that DVL-1 protein has a punctate distribution in the cell body, along the axon shaft and at the growth cone (Fig. 3, A–F). At the growth cone, the highest levels of DVL-1 were found in the central domain that contains numerous MTs (Fig. 3, D–F). In the axon shaft, DVL-1 immunoreactivity seems to localize to regions of the axon where MTs are present (Fig. 3 A). To visualize MTs, we used acetylated tubulin antibody that labels stable MTs (Bulinski et al., 1988). Double labeling for acetylated MTs and DVL-1 reveals that high levels of DVL-1 appear to colocalize with axonal MTs (Fig. 3, G–L). To test whether DVL-1 interacts with MTs, cerebellar granule cells were detergent-extracted during fixation, a procedure that leaves the cytoskeleton and its associated proteins intact yet removes cytoplasmic and membrane-associated proteins. DVL-1 immunoreactivity was re-

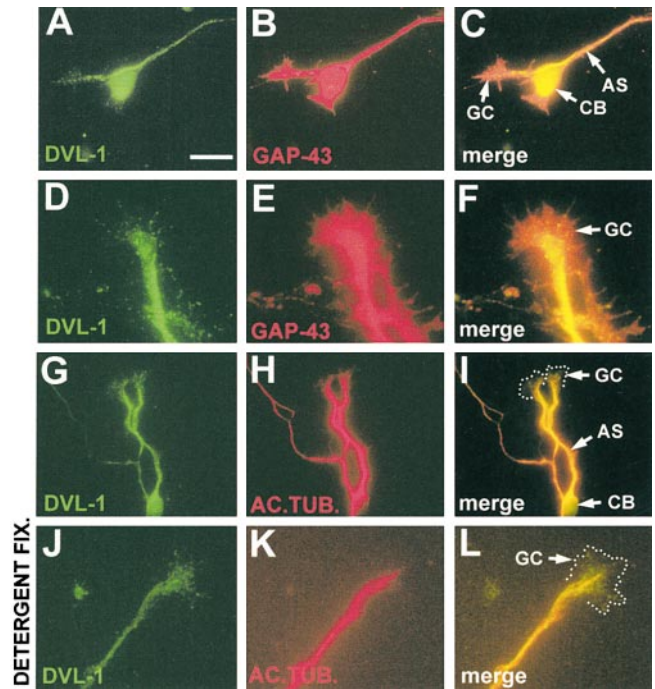


**Figure 3.** The subcellular distribution of DVL-1 in maturing cerebellar granule cell neurons. Granule cell cultures were grown for 2 d and stained with antibodies to DVL-1 (A, D, G, and J), GAP-43 (B and E), and acetylated tubulin (H and K). DVL-1 has a punctate distribution in the neuronal cell bodies and along the axon shaft (A–C). High levels of DVL-1 were detected in the central domain of the growth cone (D and F). DVL-1 immunostaining colocalizes with acetylated tubulin along the axon shaft (G–I). In neurons fixed in the presence of detergent, a pool of DVL-1 remains colocalized with acetylated tubulin (J–L). CB, cell body; AS, axon shaft; GC, growth cone. Bar: A–C and G–I, 20  $\mu$ M; D–F and J–L, 10  $\mu$ M.

tained after detergent extraction, although at a lower level, suggesting that a fraction of DVL-1 is associated with the cytoskeleton (Fig. 3, J–L). In contrast, the membrane-bound protein, GAP-43, was removed by this treatment (data not shown). Most of the DVL-1 immunoreactivity colocalizes with acetylated MTs (Fig. 3, J–L). However, at the growth cone, low levels of DVL-1 were found in areas lacking acetylated MTs, suggesting that DVL-1 may also be associated with other cytoskeleton components (Fig. 3, J–L). These results suggest that a pool of DVL-1 colocalizes with axonal MTs.

To investigate the possible association of DVL-1 with axonal MTs, we examined whether endogenous DVL-1 cosediments with taxol-polymerized MTs from mice brain. Indeed, DVL-1 was found in taxol-stabilized MT fractions (Fig. 4, A and B). In adult brain lysate, similar levels of the 83-kD isoform were found in the soluble and pellet fractions when taxol was absent (Fig. 4 A). Addition of taxol leads to MT polymerization and sedimentation of most of the 83-kD protein into the pellet MT fraction (Fig. 4 A). We also examined the distribution of endogenous DVL-1 at early postnatal stages when all three isoforms of DVL-1 are present. The soluble fraction from P5 brain contains low levels of the 96-kD DVL-1 protein. However, MT fractions contain the 88-kD pro-

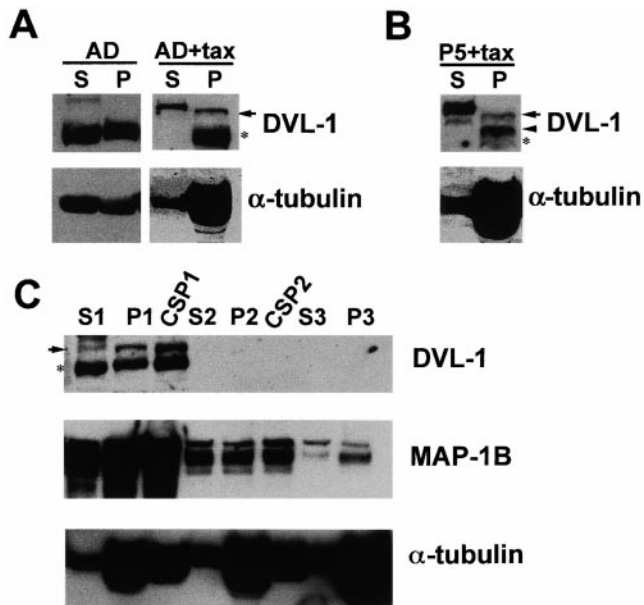


**Figure 4.** DVL-1 cosediments with stabilized microtubules. (A) In adult brain lysate, the endogenous 83-kD DVL-1 isoform is equally distributed between supernatant (S) and pellet (P) fractions (AD). In the presence of taxol, the 83-kD isoform (asterisk) becomes more abundant in the stabilized MT pellet (P) with low levels of the 96-kD isoform (arrow; AD+tax). The high molecular weight band in the soluble fraction of taxol-treated lysate is not specific. Reprobing for  $\alpha$ -tubulin reveals an enrichment of MTs in the pellet fraction from taxol-containing samples. (B) In P5 brain samples treated with taxol, high levels of the 88-kD DVL-1 protein (arrowhead) and low levels of the 96-kD (arrow) and 83-kD (asterisk) DVL-1 proteins are detected in the taxol-MT pellet (P). Low levels of the 96-kD isoform is found in the soluble fraction (S). Reprobing for  $\alpha$ -tubulin reveals an enrichment of MTs in the pellet fraction of taxol-treated lysates. (C) DVL-1 cosediments with the cold stable MT pellet from adult brain. High levels of the 83-kD (asterisk) and low levels of the 96-kD (arrow) DVL-1 proteins were found in the soluble (S1) and MT fractions (P1). After a round of depolymerization, DVL-1 is most abundant in the cold-stable MT pellet (CSP1). No DVL-1 was detected with MT fractions in subsequent cycles of polymerization. High levels of MAP-1B cosediment with the cold-stable MT pellet (CSP1), whereas low levels of MAP-1 are found after MT cycling (P2 and P3).

tein and low levels of the 96- and 83-kD DVL-1 proteins (Fig. 4 B). These results show that a higher proportion of DVL-1 becomes associated with MTs in adult brain compared with younger brain (compare Fig. 4, A and B).

To test further the association of DVL-1 with MTs, we performed MT depolymerization and repolymerization experiments in which MTs are depolymerized by cold temperature and repolymerized by GTP at 37°C. After polymerization of MTs from adult brain lysate, the 96-kD isoform and, more abundantly, the 83-kD DVL-1 isoform cosediment with polymerized MTs (Fig. 4 C). However, the 83-kD DVL-1 protein was also found in the soluble fraction (S1). Interestingly, when the MT pellet (P1) was subjected to another round of depolymerization, high levels of the DVL-1 immunoreactivity were found in the cold stable MT pellet. Cold stability is a property of neuronal MTs that have a high proportion of stable MTs (Webb and

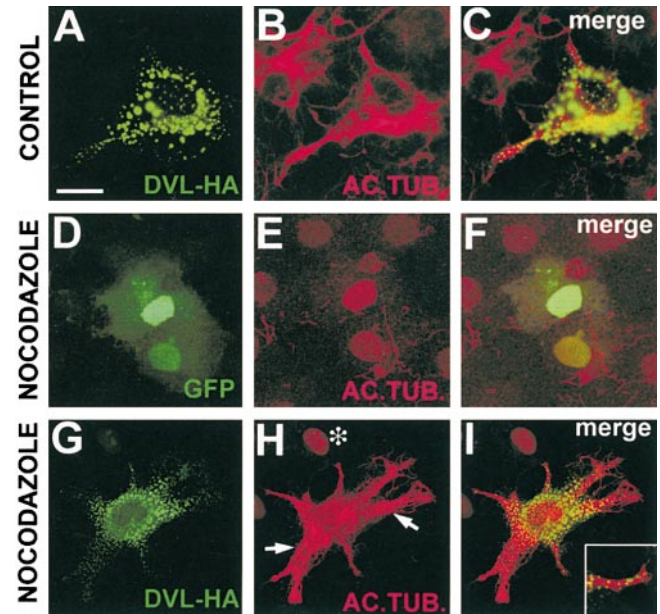


**Figure 5.** DVL-1 prevents the loss of stable microtubules in nocodazole treated COS-7 cells. COS-7 expressing DVL-HA (A–C and G–I) or GFP (D–F) were examined for the level of MTs (B, E, and H). COS-7 cells expressing DVL-HA (A) have a normal level of acetylated MTs (B and C). COS-7 cells expressing GFP (D–F) or DVL-HA (G–I) were treated with nocodazole to depolymerize MTs. GFP-expressing cells have no acetylated MTs, similar to neighboring untransfected cells (D–F). Expression of DVL-HA prevents MT depolymerization by nocodazole (G–I). Arrows denote MTs resistant to nocodazole in the cell expressing DVL-HA. \*Neighboring untransfected cell, which has lost stable MTs. (Inset) Small vesicle-like structures are present on some MTs. Bar, 50  $\mu$ M.

Wilson, 1980). These findings suggest that DVL-1 is tightly associated with the more stable pool of MTs (Fig. 4 C). In further cycles, no DVL-1 was detected (Fig. 4 C). In contrast, the MT-associated protein, MAP-1B, cosediments with MTs after a few cycles of depolymerization/repolymerization (Fig. 4 C), although at much lower levels in the second and third cycles (Fig. 4 C). The lack of detection of DVL-1 in further cycles could be due to the low levels of endogenous DVL-1 in brain samples as compared with MAP-1B. To test this possibility, we added exogenous DVL-1 protein to the crude MT fraction. We found that addition of a lysate from DVL-HA-expressing COS cells increases the level of DVL-1 in the cold stable pellet; however, no DVL-1 was detected in the second cycle of polymerization (data not shown). Taken together, these experiments show that endogenous DVL-1 protein, especially the 83-kD isoform, is associated with taxol-stabilized MT fractions and with cold-stable MTs from the adult brain.

### DVL-1 Stabilizes Microtubules

The interaction of endogenous DVL-1 with neuronal MTs suggests its possible role in controlling MT organization or, alternatively, that MTs are just used to transport DVL-1 along the axon. We obtained evidence in favor of the former possibility when we examined the effect of expression of *Dvl-HA* on MTs in COS cells. Consistent with re-

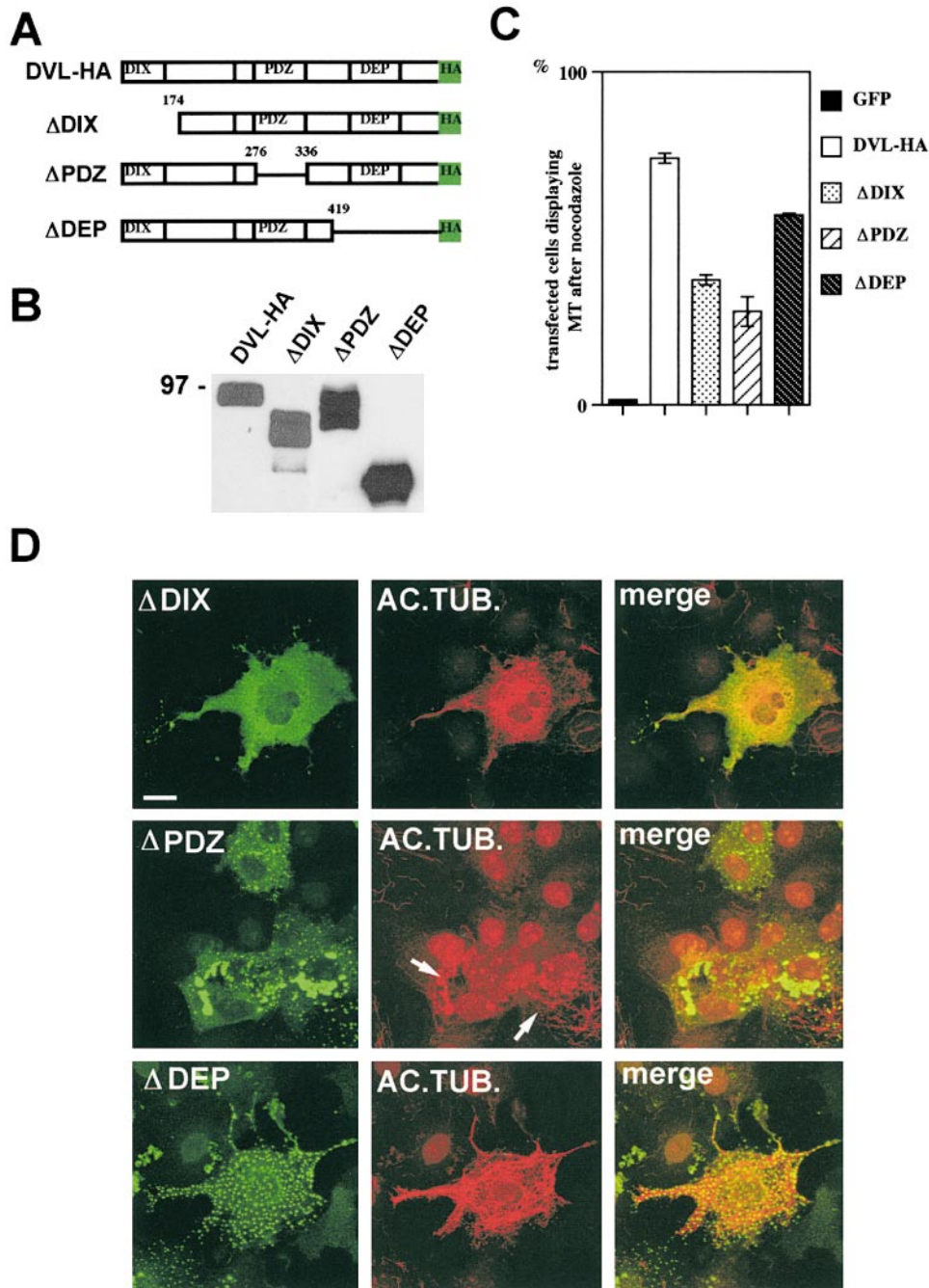


**Figure 6.** Microtubule stabilization by DVL-1 requires the PDZ domain. (A) Schematic representation of DVL-1 full-length and deletion constructs with the conserved domains. (B) Western analysis using the anti-HA antibody shows that COS-7 cells transfected with the full length and deletion constructs express similar levels of DVL-1 proteins. (C) Quantification of the number of transfected cells containing MTs after nocodazole treatment. The error bars show mean  $\pm$  SEM (results of at least three experiments). More than 150 cells were counted in each experiment for each deletion construct. (D) COS-7 cells expressing different deletions of DVL-1 were double-immunostained for DVL-HA (green) and acetylated tubulin (red). Cells expressing  $\Delta$ DIX have some MTs after nocodazole treatment, whereas expression of  $\Delta$ PDZ confers no protection. Cells expressing  $\Delta$ DEP have similar levels of MTs as cells expressing full length DVL-1. Arrows indicate the presence of very few MTs in  $\Delta$ PDZ-expressing cells. Bar, 50  $\mu$ M.

vious studies, DVL-HA forms vesicle-like structures in transfected cells (Fig. 5, A and G; Fagotto et al., 1999; Smalley et al., 1999). Cells expressing DVL-1 have similar levels of acetylated MTs than neighboring nonexpressing cells (Fig. 5, A–C). Similar results were obtained with DVL-1 without the epitope tag HA (data not shown). We then examined the effect of DVL-1 on MTs in cells that have been treated with 10  $\mu$ M nocodazole, an MT depolymerizing drug (Hoebeke et al., 1976; Lee, 1990). Expression of GFP (control) does not prevent nocodazole-induced MT depolymerization as GFP-expressing cells, like untransfected cells, have no stable MTs (Fig. 5, D–F). However, cells expressing DVL-HA have a significant number of stable MTs after nocodazole treatment (Fig. 5, G–I). We often observed that DVL-1 induces the formation of pro-

cesses (Fig. 5, G–I). Interestingly, most of the DVL-HA that colocalizes with MTs is in small vesicle-like structures (Fig. 5 I, insert). The stabilizing effect of DVL-1 was quantified by counting the number of transfected cells displaying stable MTs after nocodazole treatment. While expression of GFP does not stabilize microtubules, DVL-HA driven by the cytomegalovirus promoter stabilizes MTs in 74.7% of transfected cells after nocodazole treatment (Fig. 6 C). These results show that DVL-1 can protect MTs from nocodazole and can therefore act as an MT stabilizer.

#### *The PDZ Domain of DVL-1 Is Required for Microtubule Stabilization*

Dishevelled proteins have three conserved domains that are required for signaling through distinct pathways

(Boutros and Mlodzik, 1999). To begin to define the domain(s) of Dishevelled necessary for MT stabilization, we generated three deletion constructs carrying the HA epitope tag at the COOH termini (Fig. 6 A). All constructs express similar levels of proteins after transfection in COS cells as detected by the HA antibody (Fig. 6 B). Analysis of nocodazole-treated COS cells shows that 74.7% of the cells expressing the full-length DVL-1 have stable MTs (Fig. 6 C). Deletion of the DIX domain, ( $\Delta$ DIX-DVL-1) confers stabilization to 34% of cells (Fig. 6, C and D) with similar numbers of MTs, as compared with full-length DVL-1 (Figs. 5 I and 6 D). Expression of  $\Delta$ PDZ-DVL-1 results in the presence of very few stable MTs in only 23% of the transfected cells. In contrast, deletion of the COOH end, containing the DEP domain, does not affect the ability of DVL-1 to stabilize MTs, as 57.5% of the cells contain high numbers of stable MTs (Fig. 6, C and D). These experiments show that the DEP domain of DVL-1 is not required for MT stabilization, while the PDZ domain and, to a lesser extent, the DIX domain are required for MT stabilization.

### The Microtubule Stabilizing Activity of DVL-1 Is Mediated through GSK-3 $\beta$

In the WNT signaling pathway, activation of Dishevelled results in the inhibition of GSK-3 $\beta$  (Cadigan and Nusse, 1997; Arias et al., 1999). GSK-3 $\beta$  itself phosphorylates a number of MT-associated proteins such as Tau, MAP-1B, and MAP-2 that control MT stability (Hanger et al., 1992; Mandelkow et al., 1992; Lucas et al., 1998). Therefore, DVL-1 might regulate MT stability through inhibition of GSK-3 $\beta$ . Consistent with this idea, expression of GSK-3 $\beta$  blocks the ability of DVL-1 to protect MTs against nocodazole (Fig. 7, A–C). This effect of GSK-3 $\beta$  depends on its kinase activity as a kinase-dead, dominant-negative form of GSK-3 $\beta$  (dnGSK-3 $\beta$ ) fails to block the MT stabilizing effect of DVL-1 (Fig. 7, D–F and J). Neither GSK-3 $\beta$ -HA nor dnGSK-3 $\beta$ HA when expressed alone have a detectable effect on MT stability in nocodazole-treated cells (data not shown). Expression of DVL-1 under the SV40 promoter prevents MT depolymerization in 65.6% of transfected cells (Fig. 7 J), whereas 15.2% of cells expressing DVL-1 and GSK-3 $\beta$ -HA display stable MTs after nocodazole treatment (Fig. 7 J). dnGSK-3 $\beta$ , when coexpressed with DVL-1, protects MTs against depolymerization by nocodazole in 74.4% of cells (Fig. 7 J). Interestingly, coexpression of dnGSK-3 $\beta$  and DVL-1 increases the number of cells that retain their MTs (Fig. 7 J), suggesting that dnGSK-3 $\beta$  enhances DVL-1 function. These results suggest that DVL-1 stabilizes MTs through the inhibition of GSK-3 $\beta$ . To test further this idea, we examined the effect of lithium, a direct inhibitor of GSK-3 $\beta$  and an activator of the WNT pathway (Klein and Melton, 1996). Control NaCl has no effect on MT stability (Fig. 7 G). In contrast, lithium chloride stabilizes MTs in COS cells treated with nocodazole (Fig. 7, H and I). Lithium has a concentration-dependent MT stabilizing effect. At 20 mM lithium, few MTs are stabilized (Fig. 7 H), whereas more MTs are stabilized in the presence of 40 mM lithium (Fig. 7 I). The addition of *myo*-inositol to lithium-treated cells did not affect the MT stabilizing effect of lithium, suggesting that depletion of inositol, another known effect of lithium (Atack et al., 1995), is not involved

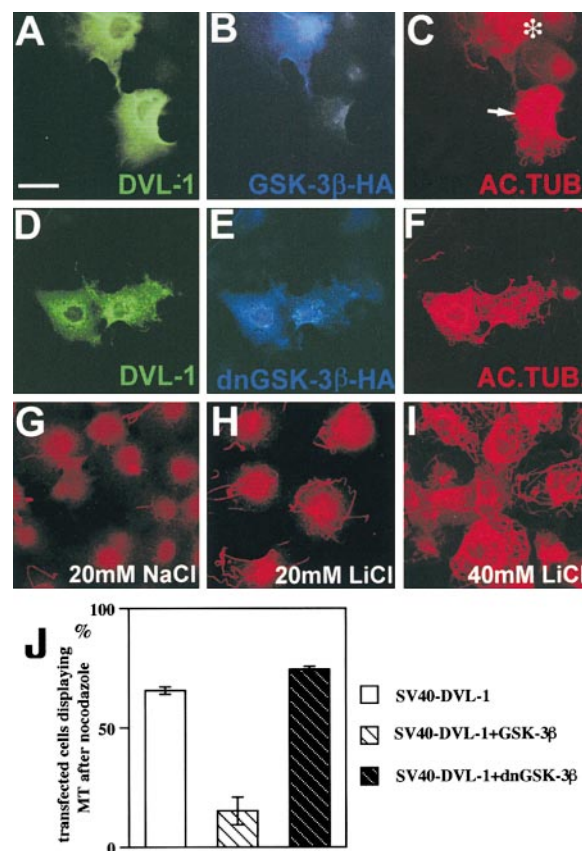


**Figure 7.** Inhibition of GSK-3 $\beta$  by DVL-1 or lithium stabilizes microtubules. (A–C) COS-7 cells double transfected with DVL-1 and GSK-3 $\beta$ -HA were treated with nocodazole. The cells were fixed and triple-stained with antibodies to DVL-1 (green), HA (blue), and acetylated tubulin (red). Cells expressing DVL-1 and GSK-3 $\beta$ -HA have very low level of acetylated MTs (asterisk), whereas a neighboring cell expressing only DVL-1 (C, arrow) contains MTs after nocodazole treatment. (D–F) Expression of the kinase-dead form of GSK-3 $\beta$  (dnGSK-3 $\beta$ -HA) in DVL-1-expressing cells does not block the ability of DVL-1 to protect MTs against nocodazole treatment. (G) COS-7 cells cultured in control NaCl-containing medium have no stable MTs after nocodazole treatment. (H) Cells treated with 20 mM LiCl have few acetylated MTs after nocodazole treatment, whereas in the presence of 40 mM LiCl (I), a larger proportion of acetylated MTs is present in nocodazole-treated cells. (J) Graph shows the percentage of cells containing MTs after nocodazole treatment. Note that expression of dnGSK-3 $\beta$  and DVL-1 results in a small but significant increase in the number of cells containing MTs (65.6% and 74.4%; *t* test, *P* < 0.005). Values are mean  $\pm$  SEM from three separate experiments. Bar, 50  $\mu$ M.

in this process (data not shown). These results suggest that the MT stabilizing activity of DVL-1 is mediated by the inhibition of GSK-3 $\beta$ .

### DVL-1 Stabilizes Axonal Microtubules

DVL-1 colocalizes with axonal MTs in maturing neurons (Fig. 3). To test whether DVL-1 also regulates the stability of axonal MTs, we examined the effect of expression of DVL-HA in differentiated NB2a neuroblastoma cells. Untransfected and GFP-expressing NB2a cells have bundles of acetylated MTs along the axon (Fig. 8, B and C, and data

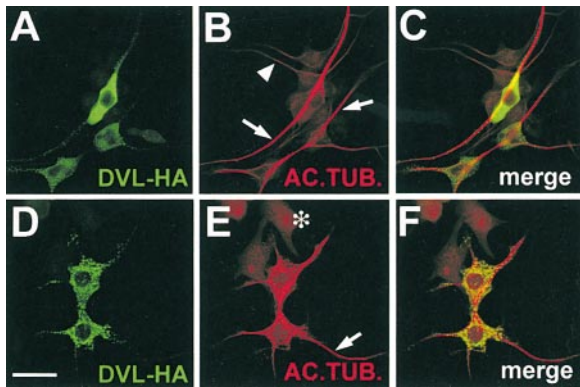


**Figure 8.** DVL-1 stabilizes axonal microtubules. (A–C) Differentiated NB2a cells expressing DVL-HA have higher levels of acetylated MTs (arrows) than untransfected neighboring cells (arrowhead). (D–F) Neurons expressing DVL-HA have acetylated MTs after nocodazole treatment (arrow), whereas untransfected cells have no acetylated MTs (asterisk). Bar, 25  $\mu$ M.

not shown). In contrast, expression of DVL-HA increases the level of acetylated MTs in NB2a neurons (Fig. 8, A–C). Treatment with nocodazole results in the loss of acetylated MTs and retraction of axons in untransfected NB2a cells (Fig. 8, E and F), whereas DVL-HA protects stable MTs from nocodazole treatment (Fig. 8, D–F), as observed in COS cells (Fig. 5, G–I). DVL-HA-expressing cells do not retract their axons in the presence of nocodazole (Fig. 8, D–F). Thus, DVL-1 increases the level of acetylated MTs and stabilizes axonal MTs against the depolymerizing effect of nocodazole. Like in COS cells, lithium treatment also results in increased MT stability (data not shown). These findings suggest that neuronal DVL-1 regulates, through GSK-3 $\beta$ , MT stability in developing axons.

## Discussion

In this paper, we demonstrate a novel function of DVL-1 in regulating MT stability. In neurons, endogenous DVL-1 colocalizes with axonal MTs and sediments with MT fractions. Our studies show that DVL-1 stabilizes MTs, a process mediated by the inhibition of GSK-3 $\beta$ . These findings suggest a possible mechanism by which Dishevelled proteins could regulate cell morphology, cell polarity, and asymmetric cell divisions.

### Dishevelled Is Associated with Microtubules

Previous studies in *Xenopus* embryos have shown that Dsh-GFP moves along MTs, suggesting that Dishevelled interacts with MTs, although biochemical evidence was not provided (Miller et al., 1999). Here we demonstrate a physical association of endogenous DVL-1 with MTs isolated from brain tissues. Consistent with these findings, DVL-1 is mainly localized to neurons that contain high levels of stable MTs. Thus, Dishevelled proteins associate with MTs in different cell types, suggesting a general role for Dishevelled in regulating MT organization.

Three isoforms of DVL-1 are expressed during postnatal cerebellar development with the 83-kD DVL-1 isoform becoming more predominant in adult cerebellum. This isoform is tightly associated with cold stable MT fractions,

representing axonal MTs (Webb and Wilson, 1980; Brady et al., 1984). In agreement with this finding, immunofluorescence studies show that DVL-1 colocalizes with MTs in developing axons. The association with cold stable MTs has been observed with STOP proteins and Doublecortin, both microtubule-associated proteins that regulate MT stability (Guillaud et al., 1998; Francis et al., 1999; Gleeson et al., 1999). DVL-1 cosediments with taxol or GTP-polymerized MTs. When brain MTs are run through cycles of depolymerization and repolymerization, most of the endogenous DVL-1 sediments with the first MT pellet and with the cold stable pellet. However, no DVL-1 was detected in further rounds of depolymerization and repolymerization even when exogenous DVL-1 protein was added. The presence of DVL-1 in the pellet after microtubule depolymerization suggests that a pool of DVL-1 is associated with cytoskeleton components, other than microtubules. Interestingly, recent studies show that DVL-1 colocalizes with actin fibers (Torres and Nelson, 2000). Alternatively, the presence of DVL-1 in the cold stable pellet may indicate a very strong association with a pool of microtubules. Microtubule-associated proteins that regulate MT stability cycle with MTs to different degrees. MAP-2 and Tau cycle well, while MAP-1B has a relatively poor cycling ability (Gordon-Weeks et al., 1995). Thus, the lack of cycling of DVL-1 should not be interpreted as a poor association with MTs. On the contrary, the presence of high levels of DVL-1 in the cold stable pellet, which represents the most stable pool of MTs, suggests that DVL-1 is tightly associated with stable MTs.

How is DVL-1 associated with MTs? DVL-1 does not have a distinguishable MT-binding domain like other MT binding proteins (Drewes et al., 1998). Therefore, DVL-1 could bind to MTs through a novel, as yet unidentified, MT binding domain. Alternatively, DVL-1 may associate indirectly with MTs by interacting with other microtubule-binding proteins. Interestingly, *Adenomatous polyposis coli* (APC), a protein that regulates WNT signaling, has a MT binding domain (Munemitsu et al., 1994; Papkoff et al., 1996; McCartney et al., 1999). APC has recently been shown to form a complex with Axin, a protein that interacts with Dishevelled (Fagotto et al., 1999; Smalley et al., 1999). As APC increases MT assembly (Munemitsu et al., 1994), DVL-1 could regulate MT dynamics by interacting with proteins such as APC. Further studies are needed to address this possibility.

### DVL-1 Stabilizes Microtubules through GSK-3 $\beta$ Inhibition

DVL-1 regulates MT stability as expression of DVL-1 increases the level of acetylated MTs and protects MTs from depolymerization by nocodazole in COS and neuroblastoma 2a cells. Similar results have been observed with microtubule-associated proteins such as Tau, MAP-1B, and MAP-2, which increase MT stability (Baas et al., 1994; Takemura et al., 1992). Thus, DVL-1 acts as a MT stabilizing factor.

How does DVL-1 regulate MT stability? Dishevelled proteins contain three conserved domains, a DIX domain also present in Axin, a negative regulator of the WNT signaling pathway, a PDZ domain present in a number of junctional proteins of the PSD-95 and Disc-large family,



and a DEP domain present in the *Caenorhabditis elegans* protein Egl-10 and in Pleckstrin (for review, see Boutros and Mlodzik, 1999). The PDZ domain is required for Armadillo stabilization through the canonical WNT pathway (Sokol et al., 1995; Yanagawa et al., 1995). In contrast, the DEP domain, but not the PDZ domain, is required for JNK signaling (Boutros et al., 1998; Li et al., 1999). Here, we show that the PDZ domain is required for MT stabilization, while deletion of the DIX domain has a weaker effect. In contrast, deletion of the DEP domain does not affect the MT stabilizing function of DVL-1. The requirement of the PDZ domain suggests that DVL-1 may be acting through the canonical pathway. Consistent with these findings, DVL-1 stabilizes MTs through the inhibition of GSK-3 $\beta$ , a downstream component of the canonical WNT pathway. This mechanism is supported by three findings. Firstly, expression of GSK-3 $\beta$  blocks the MT stabilizing activity of DVL-1. Secondly, dnGSK-3 $\beta$  enhances DVL-1 function. Thirdly, lithium, an inhibitor of GSK-3 $\beta$  (Klein and Melton, 1996), mimics the MT stabilizing activity of DVL-1. Inhibition of GSK-3 $\beta$  by DVL-1 could lead to changes in the phosphorylation of microtubule-associated proteins such as Tau, MAP-1B, and MAP-2 that are direct targets of GSK-3 $\beta$  (Hanger et al., 1992; Lucas et al., 1998; Sanchez Martin et al., 1998). Studies of Tau and MAP-1B show that GSK-3 $\beta$ -mediated phosphorylation decreases the ability of Tau to bind to MTs and decreases MT stabilization by MAP-1B (Wagner et al., 1996; Hong et al., 1997; Goold et al., 1999). Thus, inhibition of GSK-3 $\beta$  by DVL-1 may change the ability of MAPs to stabilize MTs. Although inhibition of GSK-3 $\beta$  by lithium stabilizes MTs, DVL-1 has a stronger stabilizing effect than high levels of lithium. Thus, it is likely that DVL-1 promotes MT stability via inhibition of GSK-3 $\beta$ , but an alternative pathway may also contribute to this function of DVL-1. Dishevelled has recently been found to colocalize with actin fibers (Torres and Nelson, 2000). More importantly, Dishevelled has been proposed to influence the actin cytoskeleton through the JNK pathway (Strutt et al., 1997; Axelrod et al., 1998). As MT dynamics is influenced by actin, Dishevelled could regulate MTs indirectly through the JNK pathway by changing the actin cytoskeleton. However, this mechanism seems unlikely, as the DEP domain of DVL-1, essential for the JNK pathway, is not required for MT stability. Consequently, our data suggest that MT stabilization by DVL-1 is mediated through GSK-3 $\beta$  signaling and a parallel, as yet unidentified, pathway.

In maturing neurons, endogenous DVL-1 colocalizes with axonal MTs that contain high levels of stable MTs. More importantly, DVL-1 increases the level of stable MTs in differentiated NB2a neuroblastoma cells and protects axonal MTs against nocodazole treatment. These findings suggest that neuronal DVL-1 may stabilize axonal MTs in vivo. Consistent with this view, a higher proportion of endogenous DVL-1 becomes associated with MTs from adult brain samples, which are enriched in stable MTs. Moreover, DVL-1 sediments with cold stable MT fractions representing the most stable pool of MTs. Thus, the localization of DVL-1 to MTs correlates with increased MT stability in maturing axons. Further studies are needed to address the in vivo role of DVL-1 in microtubule dynamics in developing neurons.

## Dishevelled in Cell Polarity and Movement

Dishevelled has been implicated in three processes in which the reorganization of the cytoskeleton is essential: planar polarity, cell movement, and mitotic spindle orientation. In *Drosophila*, the epithelial planar polarity mutant phenotype is characterized by the random orientation of cells within the epithelia in the wing, leg, and eye. In the wing, epithelial cells are oriented along the proximal-distal axis and each develops a hair pointing towards the distal end. Mutations in *dishevelled* or *frizzled* result in the random orientation of this hair (Adler, 1992). In the *Drosophila* eye, Fz/Dsh signaling affects mirror-symmetric arrangement of ommatidia (Cooper and Bray, 1999; Fanto and Mlodzik, 1999). Dishevelled lies upstream of RhoA/Rac and the JNK kinase pathway in the control of planar polarity in the eye and wing (Strutt et al., 1997; Boutros et al., 1998). In addition, mutational analyses have demonstrated that Armadillo/ $\beta$ -catenin or pangolin/T-cell factor are not required for planar polarity in the eye (Boutros et al., 1998). However, the role of *shaggy*, the *Drosophila* homologue of GSK-3, is less clear. Although *shaggy* mutants do not exhibit a planar polarity phenotype in the wing (Axelrod et al., 1998), overexpression studies showed that *shaggy* produces a similar but weaker planar polarity phenotype in the eye to those observed in *fz* or *dsh* (Tomlinson et al., 1997). Therefore, it is possible that Dishevelled functions through *shaggy*/GSK-3 in planar polarity depending on the cellular context.

Recent studies in *Xenopus* and zebrafish embryos have shown that wnt-11 regulates convergent extension movements through Dishevelled (Heisenberg et al., 2000; Tada and Smith, 2000; Wallingford et al., 2000). Dishevelled does not signal through the canonical pathway, as  $\beta$ -catenin or Tcf-3 are not required (Tada and Smith, 2000). Although the role of GSK-3 has not been tested in this process, the requirement of the DEP domain, but not the PDZ domain, suggests that Dishevelled is signaling through a similar pathway to that involved in *Drosophila* planar polarity.

Dishevelled also regulates the orientation of the mitotic spindle. Mutations in the *Drosophila* *dishevelled* and *frizzled* result in random orientation of the mitotic spindle in the asymmetric cell divisions during the development of mechanosensory organs (Gho and Schweisguth, 1998). In *C. elegans*, components of the Wnt pathway upstream and downstream of *dishevelled* regulate the orientation of the mitotic spindle during asymmetric cell divisions. *gsk-3*, *mom-5/fz*, and *mom-1/porc* regulate the orientation of the mitotic spindle (Schlesinger et al., 1999). Although the role of *dishevelled* has not been demonstrated in this system, these findings strongly suggest that WNT/FZ signaling through GSK-3 regulates the organization and/or orientation of MT structures. The mechanism by which the cytoskeleton is reorganized by WNT/FZ-mediated signaling remains elusive.

In the present work, we demonstrate that endogenous DVL-1 associates with axonal MTs that contain a large pool of stable MTs. DVL-1 also stabilizes MTs in dividing cells and differentiated neurons. Our data is consistent with the idea that activation of Dishevelled, depending on the cellular context, results in MT stabilization through the

inhibition of GSK-3 $\beta$ . The localization of Dishevelled to MTs may target its function within the cell. Local inhibition of GSK-3 $\beta$  by DVL-1 may result in local changes in the phosphorylation of GSK-3 $\beta$  targets that regulate MT dynamics. This novel MT stabilizing function of DVL-1 provides a possible mechanism for regulating cell polarity.

We thank Karl Willert and Roel Nusse for providing the DVL-1-GST fusion construct for antibody production, Daniel Sussman for the *Dvl-1* cDNA, Peter Klein for *GSK-3 $\beta$*  cDNA, and Tony Wynshaw-Boris and Daniel Sussman for the *DVL-1* mutant mouse. We also thank Denis Bray and Peter Baas for useful discussions and Simon Hughes and members of our lab for comments on the manuscript.

This work was supported by a grant from the Wellcome Trust.

Submitted: 21 December 1999

Revised: 7 August 2000

Accepted: 8 August 2000

## References

- Adler, P.N. 1992. The genetic control of tissue polarity in *Drosophila*. *Bioessays* 14:735–741.
- Arias, A.M., A.M. Brown, and K. Brennan. 1999. Wnt signalling: pathway or network? *Curr. Opin. Genet. Dev.* 9:447–454.
- Atack, J.R., H.B. Broughton, and S.J. Pollack. 1995. Inositol monophosphatase: a putative target for Li<sup>+</sup> in the treatment of bipolar disorder. *Trends Neurosci.* 18:343–349.
- Axelrod, J.D., K. Matsuno, S. Artavanis-Tsakonas, and N. Perrimon. 1996. Interaction between Wingless and Notch signaling pathways mediated by dishevelled. *Science* 271:1826–1832.
- Axelrod, J.D., J.R. Miller, J.M. Shulman, R.T. Moon, and N. Perrimon. 1998. Differential recruitment of Dishevelled provides signaling specificity in the planar cell polarity and Wingless signaling pathways. *Genes Dev.* 12:2610–2622.
- Baas, P.W., T.P. Pienkowski, K.A. Cimbalkin, K. Toyama, S. Bakalis, F.J. Ahmad, and K.S. Kosik. 1994. Tau confers drug stability but not cold stability to microtubules in living cells. *J. Cell Sci.* 107:135–143.
- Boutros, M., and M. Mlodzik. 1999. Dishevelled: at the crossroads of divergent intracellular signaling pathways. *Mech. Dev.* 83:27–37.
- Boutros, M., N. Paricio, D.I. Strutt, and M. Mlodzik. 1998. Dishevelled activates JNK and discriminates between JNK pathways in planar polarity and wingless signaling. *Cell* 94:109–118.
- Brady, S.T., M. Tytell, and R.J. Lasek. 1984. Axonal tubulin and axonal microtubules: biochemical evidence for cold stability. *J. Cell Biol.* 99:1716–1724.
- Bulinski, J.C., J.E. Richards, and G. Piperno. 1988. Posttranslational modifications of alpha-tubulin: deetyrosination and acetylation differentiate populations of interphase microtubules in cultured-cells. *J. Cell Biol.* 106:1213–1220.
- Cadigan, K.M., and R. Nusse. 1997. Wnt signaling: a common theme in animal development. *Genes Dev.* 11:3286–3305.
- Cooper, M.T., and S.J. Bray. 1999. Frizzled regulation of Notch signalling polarizes cell fate in the *Drosophila* eye. *Nature* 397:526–530.
- Drewes, G., A. Ebneth, and E.M. Mandelkow. 1998. MAPs, MARKs and microtubule dynamics. *Trends Biochem. Sci.* 23:307–311.
- Fagotto, F., E. Jho, L. Zeng, T. Kurth, T. Joos, C. Kaufmann, and F. Costantini. 1999. Domains of axin involved in protein–protein interactions, Wnt pathway inhibition, and intracellular localization. *J. Cell Biol.* 145:741–756.
- Fanto, M., and M. Mlodzik. 1999. Asymmetric Notch activation specifies photoreceptors R3 and R4 and planar polarity in the *Drosophila* eye. *Nature* 397:523–526.
- Francis, F., A. Koulakoff, D. Boucher, P. Chafey, B. Schaar, M.C. Vinet, G. Friocourt, N. McDonnell, O. Reiner, A. Kahn, et al. 1999. Doublecortin is a developmentally regulated, microtubule-associated protein expressed in migrating and differentiating neurons. *Neuron* 23:247–256.
- Fujii, T., A. Nakamura, Y. Ogoma, Y. Kondo, and T. Arai. 1990. Selective purification of microtubule-associated proteins 1 and 2 from rat brain using poly(L-aspartic acid). *Anal. Biochem.* 184:268–273.
- Gho, M., and F. Schweisguth. 1998. Frizzled signalling controls orientation of asymmetric sense organ precursor cell divisions in *Drosophila*. *Nature* 393:178–181.
- Gleeson, J.G., P.T. Lin, L.A. Flanagan, and C.A. Walsh. 1999. Doublecortin is a microtubule-associated protein and is expressed widely by migrating neurons. *Neuron* 23:257–271.
- Goold, R.G., R. Owen, and P.R. Gordon-Weeks. 1999. Glycogen synthase kinase 3 $\beta$  phosphorylation of microtubule-associated protein 1B regulates the stability of microtubules in growth cones. *J. Cell Sci.* 112:3373–3384.
- Gordon-Weeks, P.R., M. Johnstone, and M. Bush. 1995. Phosphorylation of microtubule-associated protein 1B and axonal growth. *Biochem. Soc. Trans.* 23:37–40.
- Guillaud, L., C. Bosc, A. Fourest-Lieuvin, E. Denarier, F. Pirollet, L. Lafanechere, and D. Job. 1998. STOP proteins are responsible for the high

- degree of microtubule stabilization observed in neuronal cells. *J. Cell Biol.* 142:167–179.
- Hall, A.C., F.R. Lucas, and P.C. Salinas. 2000. Axonal remodeling and synaptic differentiation in the cerebellum is regulated by WNT-7a signaling. *Cell* 100:525–535.
- Hanger, D.P., K. Hughes, J.R. Woodgett, J.P. Brion, and B.H. Anderton. 1992. Glycogen synthase kinase-3 induces Alzheimer's disease-like phosphorylation of tau: generation of paired helical filament epitopes and neuronal localization of the kinase. *Neurosci. Lett.* 147:58–62.
- Hatten, M.E. 1985. Neuronal regulation of astroglial morphology and proliferation *in vitro*. *J. Cell Biol.* 100:384–396.
- Heisenberg, C.-P., M. Tada, G.-P. Rauch, L. Saude, M.L. Concha, R. Geisler, D.L. Stemple, J.C. Smith, and S.W. Wilson. 2000. Silberblick/Wnt11 activity mediates convergent extension during zebrafish gastrulation. *Nature* 405:76–81.
- Hoebcke, J., G. Van Nijen, and M. De Brabander. 1976. Interaction of nocodazole (R 17934), a new antitumoral drug, with rat brain tubulin. *Biochem. Biophys. Res. Commun.* 69:319–324.
- Hong, M., D.C.R. Chen, P.S. Klein, and V.M.Y. Lee. 1997. Lithium reduces tau phosphorylation by inhibition of glycogen synthase kinase-3. *J. Biol. Chem.* 272:25326–25332.
- Klein, P.S., and D.A. Melton. 1996. A molecular mechanism for the effect of lithium on development. *Proc. Natl. Acad. Sci. USA* 93:8455–8459.
- Klingensmith, J., R. Nusse, and N. Perrimon. 1994. The *Drosophila* segment polarity gene dishevelled encodes a novel protein required for response to the wingless signal. *Genes Dev.* 8:118–130.
- Klingensmith, J., Y. Yang, J.D. Axelrod, D.R. Beier, N. Perrimon, and D.J. Sussman. 1996. Conservation of Dishevelled structure and function between flies and mice: isolation and characterization of Dvl2. *Mech. Dev.* 58:15–26.
- Lee, G. 1990. Tau protein: an update on structure and function. *Cell Motil. Cytoskeleton* 15:199–203.
- Li, L., H. Yuan, W. Xie, J. Mao, A.M. Caruso, A. McMahon, D.J. Sussman, and D. Wu. 1999. Dishevelled proteins lead to two signaling pathways. Regulation of LEF-1 and c-Jun N-terminal kinase in mammalian cells. *J. Biol. Chem.* 274:129–134.
- Lijam, N., R. Paylor, M.P. McDonald, J.N. Crawley, C.X. Deng, K. Herrup, K.E. Stevens, G. Maccaferri, C.J. McBain, D.J. Sussman, and A. Wynshaw-Boris. 1997. Social interaction and sensorimotor gating abnormalities in mice lacking Dvl1. *Cell* 90:895–905.
- Lucas, F.R., R.G. Goold, P.R. Gordon-Weeks, and P.C. Salinas. 1998. Inhibition of GSK-3 $\beta$  leading to the loss of phosphorylated MAP-1B is an early event in axonal remodelling induced by WNT-7a or lithium. *J. Cell Sci.* 111:1351–1361.
- Lucas, F.R., and P.C. Salinas. 1997. WNT-7a induces axonal remodeling and increases synapsin I levels in cerebellar neurons. *Dev. Biol.* 193:31–44.
- Mandelkow, E.M., G. Drewes, J. Biernat, N. Gustke, J. Van Lint, J.R. Vandenheede, and E. Mandelkow. 1992. Glycogen synthase kinase-3 and the Alzheimer-like state of microtubule-associated protein tau. *FEBS Lett.* 314:315–321.
- McCartney, B.M., H.A. Dierick, C. Kirkpatrick, M.M. Moline, A. Baas, M. Peifer, and A. Bejsovec. 1999. *Drosophila* APC2 is a cytoskeletonally-associated protein that regulates wingless signaling in the embryonic epidermis. *J. Cell Biol.* 146:1303–1318.
- Millar, S.E., K. Willert, P.C. Salinas, H. Roelink, R. Nusse, D.J. Sussman, and G.S. Barsh. 1999. WNT signaling in the control of hair growth and structure. *Dev. Biol.* 207:133–149.
- Miller, J.R., B.A. Rowning, C.A. Larabell, J.A. Yang-Snyder, R.L. Bates, and R.T. Moon. 1999. Establishment of the dorsal-ventral axis in *Xenopus* embryos coincides with the dorsal enrichment of dishevelled that is dependent on cortical rotation. *J. Cell Biol.* 146:427–437.
- Munemitsu, S., B. Souza, O. Muller, I. Albert, B. Rubinfeld, and P. Polakis. 1994. The APC gene product associates with microtubules *in vivo* and promotes their assembly *in vitro*. *Cancer Res.* 54:3676–3681.
- Noordermeer, J., J. Klingensmith, N. Perrimon, and R. Nusse. 1994. Dishevelled and armadillo act in the wingless signalling pathway in *Drosophila*. *Nature* 367:80–83.
- Papkoff, J., B. Rubinfeld, B. Schryver, and P. Polakis. 1996. Wnt-1 regulates free pools of catenins and stabilizes APC-catenin complexes. *Mol. Cell Biol.* 16:2128–2134.
- Perrimon, N., and A.P. Mahowald. 1987. Multiple functions of segment polarity genes in *Drosophila*. *Dev. Biol.* 119:587–600.
- Ponting, C.P., and P. Bork. 1996. Pleckstrin's repeat performance: a novel domain in G-protein signaling? *Trends Biochem. Sci.* 21:245–246.
- Ponting, C.P., C. Phillips, K.E. Davies, and D.J. Blake. 1997. PDZ domains: targeting signalling molecules to sub-membranous sites. *Bioessays* 19:469–479.
- Rothbacher, U., M.N. Laurent, I.L. Blitz, T. Watabe, J.L. Marsh, and K.W.Y. Cho. 1995. Functional conservation of the Wnt signaling pathway revealed by ectopic expression of *Drosophila dishevelled* in *Xenopus*. *Dev. Biol.* 170:717–721.
- Sanchez-Martin, C., J. Diaz-Nido, and J. Avila. 1998. Regulation of a site-specific phosphorylation of the microtubule-associated protein 2 during the development of cultured neurons. *Neuroscience* 87:861–870.
- Schlesinger, A., C.A. Shelton, J.N. Maloof, M. Meneghini, and B. Bowerman. 1999. Wnt pathway components orient a mitotic spindle in the early *C. elegans* embryo without requiring gene transcription in the responding cell. *Genes Dev.* 13:2028–2038.

- Siegfried, E., E.L. Wilder, and N. Perrimon. 1994. Components of wingless signalling in *Drosophila*. *Nature*. 367:76–79.
- Smalley, M.J., E. Sara, H. Paterson, S. Naylor, D. Cook, H. Jayatilake, L.G. Fryer, L. Hutchinson, M.J. Fry, and T.C. Dale. 1999. Interaction of Axin and Dvl-2 proteins regulates Dvl-2-stimulated TCF-dependent transcription. *EMBO (Eur. Mol. Biol. Organ.) J.* 18:2823–2835.
- Sokol, S.Y., J. Klingensmith, N. Perrimon, and K. Itoh. 1995. Dorsalizing and neuralizing properties of Xdsh, a maternally expressed *Xenopus* homolog of dishevelled. *Development*. 121:1637–1647.
- Strutt, D.I., U. Weber, and M. Mlodzik. 1997. The role of RhoA in tissue polarity and Frizzled signalling. *Nature*. 387:292–295.
- Sussman, D.J., J. Klingensmith, P. Salinas, P.S. Adams, R. Nusse, and N. Perrimon. 1994. Isolation and characterization of a mouse homolog of the *Drosophila* segment polarity gene *dishevelled*. *Dev. Biol.* 166:73–86.
- Tada, M., and J.C. Smith. 2000. *Xwn11* is a target of *Xenopus* Brachyury: regulation of gastrulation movements via Dishevelled, but not through the canonical Wnt pathway. *Development*. 127:2227–2238.
- Takemura, R., S. Okabe, T. Umeyama, Y. Kanai, N.J. Cowan, and N. Hirokawa. 1992. Increased microtubule stability and alpha-tubulin acetylation in cells transfected with microtubule-associated proteins Map1b, Map2 or Tau. *J. Cell Sci.* 103:953–964.
- Tomlinson, A., W.R. Strapps, and J. Heemskerk. 1997. Linking Frizzled and Wnt signaling in *Drosophila* development. *Development*. 124:4515–4521.
- Torres, M.A., and W.J. Nelson. 2000. Colocalization and redistribution of Dishevelled and actin during Wnt-induced mesenchymal morphogenesis. *J. Cell Biol.* 149:1433–1442.
- Tsang, M., N. Lijam, Y. Yang, D.R. Beier, A. WynshawBoris, and D.J. Sussman. 1996. Isolation and characterization of mouse Dishevelled-3. *Dev. Dyn.* 207:253–262.
- Wagner, U., M. Utton, J.M. Gallo, and C.C.J. Miller. 1996. Cellular phosphorylation of tau by GSK-3beta influences tau binding to microtubules and microtubule organization. *J. Cell Sci.* 109:1537–1543.
- Wallingford, J.B., B.A. Rowning, K.M. Vogeli, U. Rothbacher, S.E. Fraser, and R.M. Harland. 2000. Dishevelled controls cell polarity during *Xenopus* gastrulation. *Nature*. 405:81–85.
- Webb, B.C., and L. Wilson. 1980. Cold-stable microtubules from brain. *Biochemistry*. 19:1993–2001.
- Yanagawa, S.I., F. Van Leeuwen, A. Wodarz, J. Klingensmith, and R. Nusse. 1995. The dishevelled protein is modified by wingless signaling in *Drosophila*. *Genes Dev.* 9:1087–1095.
- Yang, Y., N. Lijam, D.J. Sussman, and M. Tsang. 1996. Genomic organization of mouse Dishevelled genes. *Gene*. 180:121–123.
- Zeng, L., F. Fagotto, T. Zhang, W. Hsu, T.J. Vasicek, W.L. Perry, J.J. Lee, S.M. Tilghman, B.M. Gumbiner, and F. Costantini. 1997. The mouse fused locus encodes Axin, an inhibitor of the Wnt signaling pathway that regulates embryonic axis formation. *Cell*. 90:181–192.